3-7-2018

Acidosis potentiates endothelium-dependent vasorelaxation and gap junction communication in the superior mesenteric artery.

Ipsita Mohanty
Thomas Jefferson University

Subas Chandra Parija
Orissa University of Agriculture and Technology

Sujit Suklabaidya
Institute of Life Sciences, Bhubaneswar, Odisha, India

Satish Rattan
Thomas Jefferson University

Acidosis potentiates endothelium-dependent vasorelaxation and gap junction communication in the superior mesenteric artery

Ipsita Mohanty[a,b], Subas Chandra Parija[b], Sujit Suklabaidya[c] and Satish Rattan[a*]

[a]*Department of Medicine, Division of Gastroenterology and Hepatology, Jefferson Medical College, Thomas Jefferson University, Philadelphia, Pennsylvania*

[b]*Department of Pharmacology and Toxicology, College of Veterinary Sciences and Animal Husbandry, Orissa University of Agriculture and Technology, Bhubaneswar-751003, Odisha, India*

[c]*Tumor Microenvironment and Animal Models Laboratory, Institute of Life Sciences, Bhubaneswar, Odisha, India*

Corresponding Author

Dr. Satish Rattan,

Professor of Medicine;

Department of Medicine, Division of Gastroenterology &Hepatology,

1025 Walnut Street, Room # 320 College,

Philadelphia, PA 19107;

Email: satish.rattan@jefferson.edu

Tel # (215) 955-5614

ABSTRACT

Extracellular pH is an important physiological determinant of vascular tone that is normally maintained within 7.35-7.45. Any change outside this range leads to severe pathological repercussions. We investigated the unknown effects of extracellular acidosis on relaxation in the superior mesenteric artery (SMA) of goat. SMA rings were employed to maintain isometric contractions at extracellular pH (pH_o) 7.4 and 6.8. We analyzed the effect of acidosis (pH_o 6.8) compared to physiological pH (pH_o 7.4) on three signaling mediators of endothelium-dependent hyperpolarization: nitric oxide (NO), prostaglandin I_2 (PGI_2), and myoendothelial gap junctions (MEGJ). NO and cyclic guanosine monophosphate (cGMP) levels were compared between normal and acidic pH. Quantitative real-time PCR (qPCR) studies determined the change in expression of vascular connexin (Cx), *Cx37*, *Cx40*, and *Cx43*. Under acidosis, acetyl choline-induced relaxation was augmented in an endothelium-dependent manner via eNOS-NO-cGMP signaling. Conversely, at normal pH, acetyl choline-induced vasorelaxation was mediated primarily via COX-PGI_2 pathway. The functional activity of MEGJ was increased under acidosis as evident from increased sensitivity of connexin blockers and upregulated gene and protein expression of connexins. In conclusion, acetyl choline-induced augmented vasorelaxation under acidosis is mediated by NOS-NO-cGMP, with a partial role of MEGJ as EDH mediators in the SMA. Present data suggest a novel role of connexin as therapeutic targets to attenuate the detrimental effect of acidosis on vascular tone.

Keywords: vasorelaxation, connexin, hyperpolarization, superior mesenteric artery

1. Introduction

The superior mesenteric artery (SMA) plays a vital role in supplying blood to the large part of the gastrointestinal tract (Williams et al., 2016), and plays a direct role in the pathophysiology of the intestinal motility disorders, absorption of nutrients, and blood pressure regulation (Fleming, 2000). It carries more than 10% of the systemic output (Crimi et al., 2012). Pathological changes that reduce this output, such as diarrhea, lactic acidosis, or metabolic acidosis, may be life threatening because they can affect pH. Changes in pH are often diagnosed late and prognosis is difficult in humans and animals (Clair and Beach, 2016).

Present studies were performed in the SMA to determine the pathophysiological mechanisms and therapeutic targeting for ruminal acidosis leading to rumenitis, liver abscesses and laminitis (Penner et al., 2007). The mesenteric arteries are characterized with high sensitivity to extracellular pH (pH_o), high permeability to H^+, a rapid (< 2 min) and sustained decrease in pH, and reproducibility of the preparation of isolated arterial rings for the functional and molecular studies (Celotto et al., 2008; Mohanty et al., 2016). The SMA was selected as an *ex vivo* acidosis model for study of vasomotor changes in small ruminants at molecular and functional levels. Previous studies from our laboratory have reported an attenuated vasocontractile response under acidosis (Mohanty et al., 2016). Therefore, it was considered important to examine the effect of acidosis on mediators of vasorelaxation in the SMA.

Vascular endothelial cells (EC) express GPR4 receptor, a pH-sensing G-protein coupled receptor which detects the H^+ ion and regulates the vascular tone (Chen et al., 2011; Yang et al., 2007) by releasing different vasodilators, namely NO, prostacyclin (PGI_2), epoxyeicosanoids, anandamide, hydrogen peroxide, C-type natriuretic peptide, cytochrome P_{450}, or by activating small Ca^{2+} channels (SK_{Ca}), intermediate Ca^{2+} channels (IK_{Ca}), voltage-gated potassium

channels, ATP sensitive potassium channels (Gurevicius et al., 1995) or by a combination of these mediators (Ishizaka and Kuo, 1996). The mechanisms regulating acidosis-mediated relaxation are often complex, contradictory, and inconclusive (Celotto et al., 2008). They tend to vary with respect to neurohumoral mechanisms (Standen and Quayle, 1998), species, strain, vessels (Smith et al., 1998), and acidosis model (de Wit and Griffith, 2010). The present study examined for the first time the influence of acidic pH on the mediators of relaxation in goat SMA, a model directly relevant in understanding the pathophysiology and novel therapeutic strategies of ruminal disorders.

Despite its heterogeneity, mechanisms underlying the vascular smooth muscle cell (VSMC) relaxation following acidosis are not clear. The hyperpolarization of VSMC induced by simple current transfer from the adjacent endothelium through myoendothelial gap junctions (MEGJ) consisting of connexin (*Cx*) plays a key role in the vasorelaxation (de Wit and Griffith, 2010). It is conceivable that vascular tissues expressing specified *Cx* isoforms are modulated under acidosis, a condition especially prevalent among stall-fed ruminants. The present study aims to investigate the role of eNOS-NO-cGMP and COX-PGI_2 in relation to MEGJ in mediating endothelium-dependent hyperpolarization (EDH) in SMA under acidosis compared with the physiological pH.

2. Materials and methods

2.1. Investigational compounds

We employed the following drugs for isometric contraction studies and Griess assays: noradrenaline (NA) (Merck, Kenilworth, NJ); NG-nitro-L-arginine methyl ester, indomethacin, 1H-[1,2,4]oxadiazolo[4,3-a]quinoxalin-1one or ODQ (Cayman Chemical Co., Ann Arbor, MI);

acetyl choline (Himedia, Mumbai, India.); 18β glycyrrhetinic acid or 18β GA (MP Biochemicals, Santa Ana, CA); phosphoric acid, N-(1-naphthyl) ethylenediaminedihydrochloride, sulfanilamide, sodium nitrite, 3-Isobutyl-1-methylxanthine or IBMX (Sigma-Aldrich, St. Louis, MO); sodium nitroprusside (LOBA Chemie, Mumbai, India); 1,2-bis(2-aminophenoxy)ethane-*N*,*N*,*N*′,*N*′-tetracetate or BAPTA-AM (Life Technologies, Eugene, OR). All the solutions were prepared fresh in triple distilled water except for 18βGA, ODQ and BAPTA-AM which were dissolved in dimethyl sulfoxide (DMSO), and indomethacin, which was dissolved in ethanol.

For qPCR study, we used a 100bp DNA ladder, 1x gel loading dye, acrylamide, ammonium persulfate, chloroform, ethidium bromide (SRL); diethyl pyrocarbonate (DEPC) (Genetix, New Dehli, India); dNTPs, high capacity cDNA synthesis kit, multi scribe reverse transcriptase, SYBR Green, Taq DNA polymerase (Applied Biosystems, Foster City, CA); isopropanol (Merck); nuclease free water (Promega, Madison, WI); RNAase Zap, RNA*later* (Life Technologies, Carlsbad, CA); and Trizol reagent (ThermoFisher Scientific, Carlsbad, CA).

For immunonoblot studies, we used rabbit polyclonal Connexin 37 and Connexin 40 (Cusabio, Baltimore, MD), rabbit polyclonal Connexin 43 (Abcam, Cambridge, MA), rabbit anti-iNOS (Millipore, Lake Placid, NY), mouse anti-eNOS (BD Biosciences, San Jose, CA), mouse anti-nNOS, mouse anti-phospho eNOS (Santa cruz, Dallas, Texas) and anti-GAPDH mouse monoclonal antibody (ThermoFisher Scientific, Rockford, IL).

For cGMP assay we used cGMP detection kit (R&D Systems, Minneapolis, MN).

2.2. Methods

2.2.1. Animals

The goat mesenteric artery studies have been approved by the Institutional Animal Ethical Committee (Registration No: 433/CPCSEA/20/06/2001) vide ID130/CVS/dt.31.03.2015. Adult Black Bengal goats of 13-15 months of age and 20-25 kg in body weight were used in this study. Superior mesenteric arteries from both male and female goat were isolated and employed for this study.

2.2.2. Preparation of isolated superior mesenteric arterial rings and tension recording

After careful exposure of intestinal mesentery, a branch of the goat SMA adjacent to the duodenum and jejunum just before its splitting into inferior branch was dissected out and placed in cold aerated modified Krebs-Henseleit solution (MKHS) with the following composition (in mM): 118 NaCl, 4.7 KCl, 2.5 $CaCl_2$, 1.2 $MgSO_4$, 11.9 $NaHCO_3$, 1.2 KH_2PO_4 and 11.1 D-glucose. The solution was aerated with Carbogen (95 % O_2 + 5 % CO_2) for 20 min and then adjusted to either extracellular pH (pH_o) 7.4 or 6.8 by using 1N HCl (Celotto et al., 2011). The arteries were cleared of adventitious and connective tissues, and the endothelium was removed by cotton swab method (Rosolowsky et al., 1991).

The arterial rings of 1.5-2 mm were then mounted between two fine stainless steel L-shaped hooks and kept under a resting tension of 1.5 g in a thermostatically controlled (37.0±0.5ºC) 20 ml organ bath containing MKHS continuously aerated with Carbogen. Isometric contraction studies were performed as described previously with minor modifications (Anderson et al., 2014; Dash and Parija, 2013; Mohanty et al., 2016; Singh et al., 2016; Sharma et al., 2017). Briefly, the arterial rings were equilibrated for 90 min before recording of muscle tension, washed every 15 min (using MKHS freshly adjusted to pH 7.4 or 6.8) and the experiment repeated for both endothelium intact (ED+) and denuded (ED-) vessels wherever necessary. The change of

isometric tension was measured by a high sensitive isometric force transducer (Model: MLT0201, AD Instruments, Australia) and analyzed using chart 7.1.3 software.

2.2.3. Experimental protocol

Sub-maximal concentration of NA (10 μM) or KCl (60 mM), inferred from their concentration response curve (CRC) was used to obtain an initial phasic followed by a sustained contractile response (Mohanty et al., 2016). Acetyl choline- or sodium nitroprusside - (1 nM - 100 μM) induced vasorelaxation was elicited by its subsequent addition into organ bath at an interval of 4 min with a dose increment of 1 log unit in a cumulative manner for either ED+ or ED- SMA rings. This protocol was repeated at both pH_o 7.4 and 6.8 in SMA rings pre-incubated with 100 μM L-NAME (eNOS inhibitor) or 10 μM indomethacin (COX-inhibitor) or a combination of 100 μM L-NAME and 10 μM indomethacin or 10 μM ODQ (sGC blocker) or 10 μM ketoconazole (a cytochrome P450 inhibitor) for a period of 30 min. For certain experiments, we used 100 μM 18β GA (a gap junction inhibitor) for a period of 5 min prior to NA- (10 μM) induced contraction and acetyl choline or sodium nitroprusside -induced vasorelaxation. The percent contractile response at each concentration of acetyl choline or sodium nitroprusside was calculated by taking the net plateau tension (g) induced by NA/KCl as 100%. The percent relaxation response (E_{max} or E_{Bmax}) at each concentration was obtained by reducing percent contractile response from 100%. Percent maximal relaxation of AIR and SIR for each group was calculated using relaxation recorded at 100 μM acetyl choline (pH 6.8) and sodium nitroprusside (pH 7.4) as 100%.

2.2.4. Nitric oxide (NO) and cyclic guanosine monophosphate (cGMP) measurement

The mesenteric arterial rings (of equal weight) were incubated in normal (pH_o 7.4) and acidic (pH_o 6.8) MKHS maintained at 37°C and continuously aerated with Carbogen for 3 h. The solution in the organ bath was replenished with fresh MKHS (adjusted to pH_o 7.4 or 6.8) every 15 min, following wash. The arterial rings were homogenized in physiological buffer saline (PBS), centrifuged at 10,000 g for 40 min in 4°C. The supernatant was used for nitrite quantification by subsequent addition of Griess reagent-A (sulfanilamide) followed by Griess reagent-B (N-1-naphthyl ethylenediamine) under complete darkness and absorbance recorded within 15 min at 540 nm in spectrophotometer.

The mesenteric arterial rings were pretreated with IBMX (1 mM) for 1 h at 37°C to prevent cGMP degradation and improve assay sensitivity (Pattison et al., 2016). The SMA rings (around 1.0 g in each group) were then incubated in normal (pH_o 7.4) and acidic (pH_o 6.8) MKHS (each with 1mM IBMX) maintained at 37°C under continuous aeration for 3 h. Parallelly, SMA rings were incubated with BAPTA (1 µM, 10 µM) under normal and acidic pH to investigate the role of Ca^{2+} in activating NO-cGMP cascade. The pH of the MKHS solution was monitored every 30 mins and adjusted to pH 7.4 or 6.8 whenever needed using 1N HCl. cGMP concentrations in SMA rings perfusates were determined using an enzyme-linked immunosorbent assay (ELISA)-based cGMP detection kit in accordance with the manufacturer's instructions. All recordings were made at 540 nm and 450 nm, wavelength correction done by subtracting readings at 540 nm from 450 nm.

2.2.5. qPCR and Western blot (WB) analyses

Goat mesenteric arterial rings were incubated in normal (pH_o 7.4) and acidic (pH_o 6.8) MKHS maintained at 37°C under continuous aeration for 3 h in the same manner as for NO assay. At the

end of the incubation, the tissues were collected in RNA*later* for RNA extraction using Trizol reagent according to the manufacturer's instructions and concentration measured by Nanodrop. First-strand cDNA synthesis was performed from 2 µg of total RNA using High Capacity cDNA synthesis kit according to the manufacturer's instructions (Applied Biosystems, Foster City, CA). Gene-specific primers were designed for connexin 37 (*Cx37*), connexin 40 (*Cx40*), connexin 43 (*Cx43*) and glyceraldehyde-3-phosphate dehydrogenase (*GAPDH*) and synthesized by Eurogentec USA (Fremont, CA) (Table 1). 2 µl of each cDNA samples were used as a template for performing qPCR. Relative expression of *Cx37, Cx40, Cx43,* and *GAPDH* were analyzed by qPCR using SYBR Green (Applied Biosystems) on the MJ Research Real-time PCR System (Bio-Rad, Hercules, CA) with an annealing temperature of 50-55°C. *GAPDH* was used as an internal control. The quantification of relative fold change in connexin expression was performed using $2^{-\Delta\Delta}$Ct method.

WB studies were performed to determine a correlation between the PCR and protein expressions. The goat SMA tissues were harvested in the same manner as that for RNA extraction and were subjected to WB analysis for protein expression analysis, as described previously (Singh et al., 2016). Briefly, total protein from each sample was separated by sodium dodecyl sulfate-polyacrylamide gel electrophoresis (SDS-PAGE) and transferred to polyvinylidenedifluoride membranes (Millipore, Bedford, MA). The membranes subjected to immunoblot analysis using rabbit polyclonal Connexin 37, rabbit polyclonal Connexin 40, rabbit polyclonal Connexin 43, rabbit anti-iNOS, mouse anti-nNOS, mouse anti-eNOS, mouse anti phospho eNOS antibodies relative to anti-GAPDH mouse monoclonal antibody were imaged, as described previously (Singh et al., 2016). Densitometric analysis using ImageJ

software was conducted for the protein bands from immunoblotting to determine the relative protein expressions.

2.2.7. Statistical analysis

All values expressed as mean±S.E.M. in 'n' experiments were analyzed in Graph-Pad prism5 software (San Diego, CA) and compared using either 2 way ANOVA followed by Bonferroni's least significant difference post hoc test to make multiple comparisons or unpaired student's 't' test using GraphPad Software Quick Calcs. '*P*' value < 0.05 was considered statistically significant.

3. Results

3.1. Effect of acidic pH_o on acetyl choline (AIR) and sodium nitroprusside (SIR)-evoked relaxation and their correlation to nitric oxide (NO)

In noradrenaline (NA)-pre-contracted SMA, acetyl choline-produced a concentration-dependent vasorelaxation at pH_o 7.4, which was augmented at pH_o 6.8 with a leftward shift of CRC (Fig. 1A). Endothelium denudation (ED-) abolished acetyl choline-induced relaxation (AIR) at both pH_o 7.4 and 6.8 compared to the endothelium intact (ED+) preparations. Similarly, AIR in KCl-pre-contracted SMA rings was increased significantly ($P < 0.05$) at pH_o 6.8 compared to pH_o 7.4 (Fig. 1B). On the contrary, following NA-pre-contraction, sodium nitroprusside -induced relaxation (SIR) did not differ significantly at either pH_o (Fig. 1C).

The NO values for SMA rings increased significantly ($P < 0.05$) to 131.58±4.77% at pH_o 6.8 ($P < 0.05$) considering 100% at pH_o 7.4 (Fig. 1D). The absolute values of NO under pH_o 6.8 and pH_o 7.4 were 31.49±0.09 and 23.99±1.43 µM g^{-1}, respectively (n = 6). Thus, AIR in NA-pre-contracted ED+ SMA was potentiated with a decrease in pH_o while endothelium denudation

abolished the relaxation suggesting activation of eNOS and increased release of NO under acidosis.

3.2. Influence of eNOS and COX inhibitors on augmented AIR during acidosis in NA-pre-contracted SMA

At pH_o7.4, both indomethacin and the combination of L-NAME and indomethacin inhibited AIR with a rightward shift of CRC, but not by L-NAME alone. Under acidosis (pH_o 6.8) compared to control, AIR was inhibited by L-NAME and indomethacin used individually, and by their combined use (Fig. 2A-B). Percent inhibition by the blockers was calculated based on the formula [{E_{max} - E_{Bmax}/E_{max}}× 100] (Volpe et al., 2014). Percent maximal inhibition by L-NAME, indomethacin, and combination of L-NAME and indomethacin, revealed an increase in inhibition following acidosis (Fig. 2C-D). Simultaneously, the pEC_{50} of both L-NAME and indomethacin was significantly ($P < 0.05$) increased under acidosis (5.88±0.39 at pH_o 7.4 vs. 6.95±0.31 at pH_o 6.8). These data suggest that the SMA relaxation is mediated by COX-PGI_2 at physiological pH, while at acidic pH it involves both COX-PGI_2 and eNOS-NO.

3.3. Influence of eNOS and COX inhibitors on augmented AIR during acidosis in KCl-pre-contracted SMA

At pH_o 7.4, AIR was inhibited in the presence of indomethacin and combination of L-NAME and indomethacin, but not by L-NAME alone. In contrast however, at pH_o 6.8 both L-NAME, and a combination of L-NAME and indomethacin inhibited AIR (Fig. 3A-B). In resemblance with the NA-precontracted data, percent maximal inhibition by L-NAME, indomethacin, and combination of L-NAME and indomethacin was increased under acidosis (Fig. 3C-D). Comparing the pEC_{50} value of L-NAME and indomethacin (6.51±0.28 at pH_o 7.4 vs. 5.86±0.18

at pH_o 6.8) revealed an increase in the potency of combination of L-NAME and indomethacin under acidosis. Consequently, acidosis increased the AIR due to increased release of EDH mediators.

Considering the pattern of responses to above inhibitors, and that AIR was more pronounced in NA-pre-contracted preparations, further mechanistic studies were performed in the NA-pre-contracted SMA.

3.4. Role of NO-cGMP and myoendothelial gap junctions (MEGJ) on augmented AIR during acidosis

ODQ and 18β GA inhibited AIR with a rightward shift of CRC at both pH_o 7.4 and 6.8 (Fig. 4A-B), with an (Fig. 4C-D). In addition, data revealed a significant increase in percent maximal inhibition of AIR under acidosis, thus implying an increase in the potency of both ODQ and 18β GA under acidosis. These suggest the predominant role of the sGC-cGMP and gap junctions in the mediation of EDH in SMA.

Additional studies with cGMP assay revealed a significant increase in the cGMP levels in the SMA rings at pH_o 6.8 ($P < 0.05$) in comparison to the values at pH_o 7.4 (Fig. 4E). The absolute values of cGMP under pH_o 7.4 and pH_o 6.8 were 0.79±0.06 and 1.21±0.07 pmol ml^{-1}, respectively (n = 4).

3.5. Role of NO-cGMP and myoendothelial gap junctions (MEGJ) on sodium nitroprusside - induced relaxations (SIR) during acidosis

Both ODQ and 18β GA inhibited sodium nitroprusside -induced relaxation (SIR) at both pH_o 7.4 and pH_o 6.8 as compared to their respective controls (Fig. 5A-B). Comparing the % maximal inhibition at 10μM of SIR (38.96±7.33 at pH_o 7.4 vs. 56.37±4.23 at pH_o 6.8) and pEC_{50} values

(5.82±0.19 at pH_o 7.4 vs. 7.23±0.2 at pH_o 6.8), we observed an increased sensitivity of ODQ under acidosis (Fig. 5C). Similarly, 18β GA inhibited the SIR at both pH_o levels, with a significant increase in % maximal inhibition at 1μM of SIR (65.58±6.91 at pH_o 7.4 vs. 100.00±5.95 at pH_o 6.8) and pEC_{50} (5.98±0.06 at pH_o 7.4 vs. 6.94±0.13 at pH_o 6.8) under acidosis (Fig. 5D). These increase in the inhibitory potencies of ODQ and 18β GA under acidosis suggests an increased contribution of sGC-cGMP and MEGJ in the SMA relaxation.

3.6. qPCR and Western blot data

qPCR results revealed an upregulated gene expression for *Cx37, Cx40* and *Cx43* under reduced pH (Fig. 6A) in the order of *Cx37>Cx40<Cx43*.

To further determine whether these increase in the transcriptional levels translated into increase in the corresponding proteins, WB studies revealed a significant increase in *Cx37* and *Cx43* protein expression in the SMA under acidic pH, but not Cx40 ($P < 0.05$; Fig. 6B-C). Parallely, we observed a significant increase in iNOS expression under acidosis ($P < 0.05$). Western blot data was analyzed as integrated optical density (as ratios of GAPDH).

4. Discussion

These studies reveal for the first time the underlying signaling cascade following acidosis in SMA relaxation, as depicted in the model in Fig. 7. Acidic pH augments the AIR in an endothelium-dependent manner, primarily via eNOS-NO-cGMP pathway, in contrast with the physiological pH (COX-PGI_2 pathway). The functional role of MEGJ in SMA relaxation is increased at acidic pH associated with the upregulation of connexins. This suggests that acidosis-induced augmented vasorelaxation is mediated via different ions and second messengers that are

linked to NO signaling is associated with an increased number of gap junctions through upregulation of certain connexins.

Acetyl choline acting on muscarinic type 3 receptor subtype stimulates endothelium-dependent NO release (Celotto et al., 2008; Shi et al., 2011; Shi and Sarna, 2004). NO then binds to sGC to induce smooth muscle relaxation through PKG-cGMP pathway (Andreopoulos and Papapetropoulos, 2000; de Wit and Griffith, 2010; Hutcheson et al., 1999; Li et al., 2004; Murthy, 2006; Rattan and Thatikunta, 1993; Rattan and Chakder, 1992). In the present studies, a limited amount of AIR in NA pre-contracted ED+ in goat SMA rings may be species-specific (Dash and Parija, 2013). This effect is apparently endothelium-dependent (considering complete abolition of acetyl choline relaxation in ED-rings at either pH), indicating eNOS or PGI_2 as the mediators for NO release. Our data involving eNOS at normal pH in SMA, resistant to L-NAME, but sensitive to indomethacin, suggest that L-NAME may stimulate COX-2 to produce PGI_2-induced relaxation through the COX-PGI_2 pathway (Cohen et al., 1997; Dong et al., 1997; Hayashi et al., 1994; Ignarro et al., 1985). AIR on KCl pre-contracted tissues is attenuated in the presence of L-NAME and indomethacin, ruling out the role of K^+ ions in the mediation of EDH at physiological pH as K^+-depolarization is known to prevent the EDH response. This phenomenon has been described before in different systems (Cohen et al., 1997; Dong et al., 1997; Hayashi et al., 1994; Ignarro et al., 1985), via yet unidentified mechanism.

Previously published studies have shown that MEGJs play a significant role in the mediation of vasorelaxation by activating inwardly rectifying K^+ channels and/or the Na^+-K^+-ATPase (Mathewson and Dunn, 2014). Lack of effect of ketoconazole on AIR in the SMA at normal or acidic pH (data not shown) rules out the contribution of cytP450, suggesting MEGJ as the potential mediator of EDH. This effect of MEGJ is influenced by PGI_2-NO signaling (Griffith et

al., 2004). Speculatively, connexins are polymerized to organize MEGJ transmitting EDH signaling from endothelium to VSMC, and that an interference of formation of MEGJ by connexin uncouplers results in attenuation of AIR. This mechanism is supported from previous reports in SMA of rodents (Hilgers and De Mey, 2009; Sandow and Hill, 2000; Shimokawa and Morikawa, 2005).

Present studies further suggest an important role of NOS activation in the AIR during acidosis. These data are in agreement with those in other systems suggesting activation of NO signaling pathway under acidosis (Cencioni et al., 2013; Celotto et al., 2016; Dabertrand et al., 2012; de Wit and Griffith, 2010; Hattoriet al., 2002; Nagao and Vanhoutte, 1992; Riemann et al., 2017). Acidosis elicits release of NO from vascular endothelium that plays an important role in coronary vasodilation as demonstrated in dog coronary artery (Gurevicius et al., 1995). Present data show an increase in the sensitivity of both L-NAME and ODQ (as shown by an increase in their % blocking effect of AIR) establishing the role of NOS-NO-cGMP during acidosis-induced augmented relaxation in SMA. The blocking effects of L-NAME/ODQ were calculated from their respective maximal response (E_{Bmax}) as compared with their control maximal effects (E_{max}). The effectiveness of the inhibitor was determined by comparing IC_{50} (a concentration that produces 50% decrease in maximal inhibition of AIR). An increase in the sensitivity to eNOS inhibition during acidosis may be explained through an increase in endothelial free Ca^{2+} concentration under acidosis that exceeds the threshold for activation of eNOS, thus suggesting Ca^{2+}-dependent activation of eNOS under acidosis. In addition we also observed a significant increase in the expression profile of iNOS, another possible mediator of increased NO release under acidosis. However, neither eNOS (total and phospho) nor nNOS had any change at translational level under acidosis. In these studies, exact reason for the preferential increase in

the expression of iNOS vs. e- and nNOS is not clearly understood other than that the former is easily inducible and may affect the expression of the latters under the present experimental conditions. The ultimate answer to this important issue may be in the activation assays for different NOSs under different time intervals of acidosis, not within the scope of present studies.

Data further suggest a partial role of PGI_2-NO pathway based on an increase in the blocking potency of indomethacin, combination of indomethacin, and L-NAME under acidosis, as proposed before in cultured bovine corneal endothelial cells (Cha et al., 2005), and in rat mesenteric arterial bed (Hiley et al., 1995). Similarly, following KCl-pre-contraction, an increased AIR at pH_o 6.8 is inhibited by L-NAME, or by L-NAME plus indomethacin, indicating activation of EDH signaling. Further studies however are needed to determine relative contributions of different mediators of EDH at normal versus acidic pH.

Interestingly, we observed no change in SIR at either pH_o, suggesting that the endothelium plays a pivotal role in acidosis-mediated relaxation in the SMA. Moreover, we observed an increased inhibitory effect of ODQ for endothelium-dependent as well as increased potency of ODQ for endothelium-independent relaxation under acidosis, possibly via increased binding affinity of ODQ to sGC, as suggested before (Dasgupta et al., 2015). This indicates the role of NO-sGC-cGMP in the acidosis induced augmented AIR. We observed a significant increase in the release of cGMP under acidosis through ELISA which was blocked by BAPTA (1 μM, 10 μM), an intracellular Ca^{2+} chelator (Khan and Joseph, 2010), thus suggesting activation of Ca^{+2}-eNOS-NO-cGMP pathway in our model as suggested in other systems (Devika and Jaffar Ali, 2013).

Our studies further suggest an increased sensitivity of MEGJ to the connexin uncouplers, and increased expression of connexins, as proposed before during ischemia (Peracchia, 2004;

Davidson et al., 2012). In support of these phenomena, our studies show an increase in the blockade by the connexin uncouplers via both endothelium-dependent and endothelium independent pathways, during acidosis. It has been proposed that undocked hemichannels or connexon (hexamer of connexin), which are normally closed, open following exposure to stress (Bol et al., 2013). This may allow the passage second messengers and mediators of vasorelaxation (up to 1.5 kDa molecules) to synergistically pass through gap junctions leading to vascular dysfunction, as previously suggested (Davidson et al., 2012; Hiley et al., 1995; Peracchia, 2004). Furthermore, we observed that connexin inhibitors had no significant effect on AIR in ED-rings at either pH (data not shown). These data demonstrate that connexin inhibitor interfere with gap junction communication only in ED+, suggesting an involvement of MEGJ as a hyperpolarization factor in SMA.

Gap junctions are formed by connexin *37*, *40, 43*, and *45*, but only *Cx37, Cx40,* and *Cx43* are localized to EC borders (Gabriels and Paul, 1998; Inai and Shibata, 2009). To the best of our knowledge, no information is available on the effect of acidic pH on *Cx* protein in SMA. Our qPCR results revealed distinct upregulation of *Cx37 and Cx43* under acidic stress. This increased expression following a short incubation (3 h) may be explained on the basis of short half-life of connexin (1-5 h), which modulates the cell-cell communication (Liu et al., 2012; Martin and Prince, 2008; Segretain and Falk, 2004). Gel analysis of qPCR products indicates *Cx37, Cx40* and Cx*43* are widely expressed in SMA. These *Cx* are involved in the promulgation of hyperpolarization waves along the MEGJ to the SM layer, as previously suggested (Figueroa et al., 2003; Chaytor et al., 2005). Furthermore, *Cx40* itself has been shown to be involved in the basal release of NO and cyclooxygenase products, and in the regulation of acetyl choline sensitivity by *Cx40*-eNOS interaction (Meens et al., 2015). Importantly, the upregulated rank

order of gene expression of connexin in our model correlates with the functional data. Further studies examining the translational expressions confirmed that the increase in the gene expressions of Cx37 and 43.

In conclusion, AIR in the SMA is endothelium-dependent via the COX-PGI_2 pathway at normal pH, and acidosis augments this relaxation with an additional participation of NOS-NO-cGMP and MEGJ. These studies have strong implications in the pathophysiology and therapeutic targeting for acidosis-associated gastrointestinal and metabolic disorders.

Funding

Studies were supported by Department of Science and Technology, Gov. of India [INSPIRE Fellowship, IF130735] to Ipsita Mohanty; National Institutes of Diabetes and Digestive and Kidney Diseases [Grant RO1DK035385] and an institutional grant from Thomas Jefferson University to Dr. Satish Rattan.

Acknowledgments

Authors thank Dr S Senapati, ILS, India for the laboratory facilities to conduct qPCR; Dr Suresh K. Joseph, Dept Pathology & Cell Biology, Thomas Jefferson University for providing BAPTA-AM; Dr Adam Snooks, Pharmacology & Experimental Therapeutics, Thomas Jefferson University for valuable suggestions on cGMP assay; Dr Xinliang Ma, Emergency Medicine, Thomas Jefferson University for providing eNOS and iNOS antibodies.

Conflict of Interests

The authors declare that they have no competing interests.

References

Anderson, C.D., Jr., Kendig, D.M., Al-Qudah, M., Mahavadi, S., Murthy, K.S., Grider, J.R., 2014. Role of various kinases in muscarinic M_3 receptor-mediated contraction of longitudinal muscle of rat colon. J. Smooth Mus. Res. 50, 103-119.

Andreopoulos, S., Papapetropoulos, A., 2000. Molecular aspects of soluble guanylyl cyclase regulation. Gen. Pharmacol. 34, 147-157.

Bol, M., Van Geyt, C., Baert, S., Decrock, E., Wang, N., De Bock, M., Gadicherla, A.K., Randon, C., Evans, W.H., Beele, H., Cornelissen, R., Leybaert, L., 2013. Inhibiting connexin channels protects against cryopreservation-induced cell death in human blood vessels. Eur. J. Vasc. Endovasc. Surg. 45, 382-390.

Celotto, A.C., Capellini, V.K., Baldo, C.F., Dalio, M.B., Rodrigues, A.J., Evora, P.R., 2008. Effects of acid-base imbalance on vascular reactivity. Braz. J. Med. Biol. Res. 41, 439-445.

Celotto, A.C., Restini, C.B., Capellini, V.K., Bendhack, L.M., Evora, P.R., 2011. Acidosis induces relaxation mediated by nitric oxide and potassium channels in rat thoracic aorta. Eur. J. Pharmacol. 41, 88-93.

Celotto,A.C., Ferreira,L.G., Capellini,V.K., Albuquerque,A.A., Rodrigues,A.J., Evora,P.R., 2016. Acute but not chronic metabolic acidosis potentiates the acetylcholine-induced reduction in blood pressure: an endothelium-dependent effect. Braz.J.Med.Biol.Res. 49, e5007.

Cencioni,C., Melchionna,R., Straino,S., Romani,M., Cappuzzello,C., Annese,V., Wu,J.C., Pompilio,G., Santoni,A., Gaetano,C., Napolitano,M., Capogrossi,M.C., 2013. Ex vivo acidic preconditioning enhances bone marrow ckit+ cell therapeutic potential via increased CXCR4 expression. Eur.Heart J. 34, 2007-2016.

Cha, S.H., Park, J.E., Kwak, J.O., Kim, H.W., Kim, J.B., Lee, K.Y., Cha, Y.N., 2005. Attenuation of extracellular acidic pH-induced cyclooxygenase-2 expression by nitric oxide. Mol. Cell. 19, 232-238.

Chaytor, A.T., Bakker, L.M., Edwards, D.H., Griffith, T.M., 2005. Connexin-mimetic peptides dissociate electrotonic EDHF-type signalling via myoendothelial and smooth muscle gap junctions in the rabbit iliac artery. Br. J. Pharmacol. 144, 108-114.

Chen, A., Dong, L., Leffler, N.R., Asch, A.S., Witte, O.N., Yang, L.V., 2011. Activation of GPR4 by acidosis increases endothelial cell adhesion through the cAMP/Epac pathway. PloS one e27586.

Clair, D.G., Beach, J.M., 2016. Mesenteric Ischemia. N. Engl. J Med. 374, 959-968.

Cohen, R.A., Plane, F., Najibi, S., Huk, I., Malinski, T., Garland, C.J., 1997. Nitric oxide is the mediator of both endothelium-dependent relaxation and hyperpolarization of the rabbit carotid artery. Proc. Natl. Acad. Sci. U S A. 94, 4193-4198.

Crimi, E., Taccone, F.S., Infante, T., Scolletta, S., Crudele, V., Napoli, C., 2012. Effects of intracellular acidosis on endothelial function: an overview. J. Crit. Care 27, 108-118.

Dabertrand, F., Nelson, M.T., Brayden, J.E., 2012. Acidosis dilates brain parenchymal arterioles by conversion of calcium waves to sparks to activate BK channels. Circ. Res. 110, 285-294.

Dasgupta, A., Bowman, L., D'Arsigny, C.L., Archer, S.L., 2015. Soluble guanylate cyclase: a new therapeutic target for pulmonary arterial hypertension and chronic thromboembolic pulmonary hypertension. Clin. Pharmacol. Ther. 97, 88-102.

Dash, J.R., Parija, S.C., 2013. Spasmolytic effect of curcumin on goat ruminal artery is endothelium independent and by activation of sGC. Res. Vet. Sci. 95, 588-593.

Davidson, J.O., Green, C.R., Nicholson, B., O'Carroll, S.J., Fraser, M., Bennet, L., Jan Gunn, A., 2012. Connexin hemichannel blockade improves outcomes in a model of fetal ischemia. Ann. Neurol. 71, 121-132.

Devika, N.T., Jaffar Ali, B.M., 2013. Analysing calcium dependent and independent regulation of eNOS in endothelium triggered by extracellular signalling events. Mol. Biosyst. 9, 2653-2664.

de Wit, C., Griffith, T.M., 2010. Connexins and gap junctions in the EDHF phenomenon and conducted vasomotor responses. Pflug. Archiv: Eur. J. Physiol. 459, 897-914.

Dong, H., Waldron, G.J., Galipeau, D., Cole, W.C., Triggle, C.R., 1997. NO/PGI_2-independent vasorelaxation and the cytochrome P450 pathway in rabbit carotid artery. Br. J. Pharmacol. 120, 695-701.

Figueroa, X.F., Paul, D.L., Simon, A.M., Goodenough, D.A., Day, K.H., Damon, D.N., Duling, B.R., 2003. Central role of connexin40 in the propagation of electrically activated vasodilation in mouse cremasteric arterioles in vivo. Circ. Res. 92, 793-800.

Fleming, I., 2000. Myoendothelial Gap Junctions: The gap is there, but does EDHF go through it? Circ. Res. 86, 249-250.

Gabriels, J.E., Paul, D.L., 1998. Connexin43 is highly localized to sites of disturbed flow in rat aortic endothelium but connexin37 and connexin40 are more uniformly distributed. Circ. Res. 83, 636-643.

Griffith, T.M., Chaytor, A.T., Edwards, D.H., Daverio, F., McGuigan, C., 2004. Enhanced inhibition of the EDHF phenomenon by a phenyl methoxyalaninyl phosphoramidate derivative of dideoxyadenosine. Br. J. Pharmacol. 142, 27-30.

Gurevicius, J., Salem, M.R., Metwally, A.A., Silver, J.M., Crystal, G.J., 1995. Contribution of nitric oxide to coronary vasodilation during hypercapnic acidosis. Am. J. Physiol. 268, H39-H47.

Hattori, K., Tsuchida, S., Tsukahara, H., Mayumi, M., Tanaka, T., Zhang, L., Taniguchi, T., Muramatsu, I., 2002. Augmentation of NO-mediated vasodilation in metabolic acidosis. Life Sci. 71, 1439-1447.

Hayashi, K., Loutzenhiser, R., Epstein, M., Suzuki, H., Saruta, T., 1994. Multiple factors contribute to acetylcholine-induced renal afferent arteriolar vasodilation during myogenic and norepinephrine-and KCl-induced vasoconstriction. Studies in the isolated perfused hydronephrotic kidney. Circ. Res. 75, 821-828.

Hiley, C.R., Bottrill, F.E., Warnock, J., Richardson, P.J., 1995. Effects of pH on responses to adenosine, CGS 21680, carbachol and nitroprusside in the isolated perfused superior mesenteric arterial bed of the rat. Br. J. Pharmacol. 116, 2641-2646.

Hilgers, R.H.P., De Mey, J.G.R., 2009. Myoendothelial coupling in the mesenteric arterial bed; segmental differences and interplay between nitric oxide and endothelin-1. Br. J. Pharmacol. 156, 1239-1247.

Hutcheson, I.R., Chaytor, A.T., Evans, W.H., Griffith, T.M., 1999. Nitric oxide-independent relaxations to acetylcholine and A23187 involve different routes of heterocellular communication. Role of Gap junctions and phospholipase A2. Circ. Res. 84, 53-63.

Ignarro, L.J., Harbison, R.G., Wood, K.S., Wolin, M.S., McNamara, D.B., Hyman, A.L., Kadowitz, P.J., 1985. Differences in responsiveness of intrapulmonary artery and vein to

arachidonic acid: mechanism of arterial relaxation involves cyclic guanosine 3':5'-monophosphate and cyclic adenosine 3':5'-monophosphate. J. Pharmacol. Exp.Ther. 233, 560-569.

Inai, T., Shibata, Y., 2009. Heterogeneous expression of endothelial connexin (Cx) 37, Cx40, and Cx43 in rat large veins. Anat. Sci. Int. 84, 237-245.

Ishizaka, H., Kuo, L., 1996. Acidosis-induced coronary arteriolar dilation is mediated by ATP-sensitive potassium channels in vascular smooth muscle. Circ. Res. 78, 50-57.

Khan, M.T., Joseph, S.K., 2010. Role of inositol trisphosphate receptors in autophagy in DT40 cells. J. Biol. Chem. 285, 16912-16920.

Li, F., De, G.M., Rattan, S., 2004. Role of adenylate and guanylate cyclases in beta1-, beta2-, and beta3-adrenoceptor-mediated relaxation of internal anal sphincter smooth muscle. J. Pharmacol. Exp. Ther. 308, 1111-1120.

Liu, L., Gao, Z., Zhang, L., Su, L., Dong, G., Yu, H., Tian, J., Zhao, H., Xu, Y., Liu, H., 2012. Temporal dynamic changes of connexin 43 expression in C6 cells following lipopolysaccharide stimulation. Neur. Regen. Res. 7, 1947-1953.

Martin, F.J., Prince, A.S., 2008. TLR2 regulates gap junction intercellular communication in airway cells. J. Immunol. 180, 4986-4993.

Mathewson, A.M., Dunn, W.R., 2014. A comparison of responses to raised extracellular potassium and endothelium-derived hyperpolarizing factor (EDHF) in rat pressurised mesenteric arteries. PloS one 9, e111977.

Meens, M.J., Alonso, F., Le, G.L., Kwak, B.R., Haefliger, J.A., 2015. Endothelial Connexin37 and Connexin40 participate in basal but not agonist-induced NO release. Cell Commun. Signal. 13, 34.

Mohanty, I., Suklabaidya, S., Parija, S., 2016. Acidosis reduces the function and expression of α1D-adrenoceptor in superior mesenteric artery of Capra hircus. Indian J. Pharmacol. 48, 399-406.

Murthy, K.S., 2006. Signaling for contraction and relaxation in smooth muscle of the gut. Ann. Rev. Physiol. 68, 345-374.

Nagao, T., Vanhoutte, P.M., 1992. Characterization of endothelium-dependent relaxations resistant to nitro-L-arginine in the porcine coronary artery. Br. J. Pharmacol. 107, 1102-1107.

Pattison, A.M., Blomain, E.S., Merlino, D.J., Wang, F., Crissey, M.A., Kraft, C.L., Rappaport, J.A., Snook, A.E., Lynch, J.P., Waldman, S.A., 2016. Intestinal Enteroids Model Guanylate Cyclase C-Dependent Secretion Induced by Heat-Stable Enterotoxins. Infect. Immun. 84, 3083-3091.

Penner, G.B., Beauchemin, K.A., Mutsvangwa, T., 2007. Severity of ruminal acidosis in primiparous holstein cows during the periparturient period. Eur. J. Pharmacol. 90, 365-375.

Peracchia, C., 2004. Chemical gating of gap junction channels; roles of calcium, pH and calmodulin. Biochim. et Biophys. Acta. 1662, 61-80.

Rattan, S., Chakder, S., 1992. Role of nitric oxide as a mediator of internal anal sphincter relaxation. Am. J. Physiol. 262, G107-G112.

Rattan, S., Thatikunta, P., 1993. Role of nitric oxide in sympathetic neurotransmission in opossum internal anal sphincter. Gastroenterology 105, 827-836.

Riemann, A., Reime, S., Thews, O., 2017. Tumor Acidosis and Hypoxia Differently Modulate the Inflammatory Program: Measurements In Vitro and In Vivo. Neoplasia. 19, 1033-1042.

Rosolowsky, M., Pfister, S.L., Buja, L.M., Clubb, F.J., Jr., Campbell, W.B., 1991. Method of removal of aortic endothelium affects arachidonic acid metabolism and vascular reactivity. Eur. J. Pharmacol. 193, 293-300.

Sandow, S.L., Hill, C.E., 2000. Incidence of myoendothelial gap junctions in the proximal and distal mesenteric arteries of the rat is suggestive of a role in endothelium-derived hyperpolarizing factor-mediated responses. Circ. Res. 86, 341-346.

Segretain, D., Falk, M.M., 2004. Regulation of connexin biosynthesis, assembly, gap junction formation, and removal. Biochim. et Biophys. Acta 1662, 3-21.

Sharma, A., Nakade, U.P., Choudhury, S., Yadav, R.S., Garg, S.K., 2017. Extra and intracellular calcium signaling pathway(s) differentially regulate histamine-induced myometrial contractions during early and mid-pregnancy stages in buffaloes (Bubalus bubalis). An. Reprod. Sci. 179, 10-19.

Shi, X.Z., Lin, Y.M., Powell, D.W., Sarna, S.K., 2011. Pathophysiology of motility dysfunction in bowel obstruction: role of stretch-induced COX-2. Am. J. Physiol.-Gastrointest. Liver Physiol. 300, G99-G108.

Shi, X.Z., Sarna, S.K., 2004. G protein-mediated dysfunction of excitation-contraction coupling in ileal inflammation. Am. J. Physiol.-Gastrointest. Liver Physiol. 286, G899-G905.

Shimokawa, H., Morikawa, K., 2005. Hydrogen peroxide is an endothelium-derived hyperpolarizing factor in animals and humans. Life Sci. 39, 725-732.

Singh, J., Boopathi, E., Addya, S., Phillips, B., Rigoutsos, I., Penn, R.B., Rattan, S., 2016. Aging-associated changes in microRNA expression profile of internal anal sphincter smooth muscle: role of microRNA-133a. Am. J Physiol.-Gastrointest. Liver Physiol. 311(5), G964-G973.

Smith, G.L., Austin, C., Crichton, C., Wray, S., 1998. A review of the actions and control of intracellular pH in vascular smooth muscle. Cardiovas. Res. 38, 316-331.

Standen, N.B., Quayle, J.M., 1998. K^+ channel modulation in arterial smooth muscle. Acta Physiol. Scand. 164, 549-557.

Volpe, D.A., Hamed, S.S., Zhang, L.K., 2014. Use of different parameters and equations for calculation of IC(50) values in efflux assays: potential sources of variability in IC(50) determination. The AAPS Journal 16, 172-180.

Williams, K.E., Washington, M.C., Johnson-Rouse, T., Johnson, R.E., Freeman, C., Reed, C., Heath, J., Sayegh, A.I., 2016. Exogenous glucagon-like peptide-1 acts in sites supplied by

the cranial mesenteric artery to reduce meal size and prolong the intermeal interval in rats. Appetite 96, 254-259.

Yang, L.V., Radu, C.G., Roy, M., Lee, S., McLaughlin, J., Teitell, M.A., Iruela-Arispe, M.L., Witte, O.N., 2007. Vascular abnormalities in mice deficient for the G protein-coupled receptor GPR4 that functions as a pH sensor. Mol. Cell. Biol. 27, 1334-1347.

Table 1. Primers for *connexin 37, connexin 40, connexin 43* and *GAPDH* genes and their respective cycle parameters.

Receptor		**Primer sequence**	**NCBI Reference Sequence**	**Product Size (bp)**
Connexin37	Forward	TCCTTGAGAAGCTGCTAGAC	XM_005678726.1	185
	Reverse	GTCGTAGCAGACATTGGTG		
Connexin40	Forward	ATCTCCCACATTCGATACTG	XM_005677755.1	194
	Reverse	CAGGACAGCTCTGTCTTCTC		
Connexin43	Forward	ACCTGGCTCATGTGTTCTAC	XM_005684517.1	194
	Reverse	GATGTAGGTTCTCAGCAAGC		
GAPDH	Forward	GAGATCAAGAAGGTGGTGAA	XM_005680968.1	175
	Reverse	CATACCAGGAAATGAGCTTG		

Legends to Tables

Table 1. Primers for *connexin 37, connexin 40, connexin 43* and *GAPDH* genes and their respective cycle parameters.

Legends to Figures

Fig. 1. Acetyl choline but not sodium nitroprusside -induced relaxation is increased under acidosis in an endothelium-dependent manner due to increased release of nitric oxide. Acetyl choline-induced relaxation in noradrenaline- (A) and KCl (B) pre-contracted SMA is augmented at pH_o 6.8**.** AIR at pH_o 7.4 as well as pH_o 6.8 (**P* < 0.05) is nearly abolished by endothelium denudation ($^{\#}P < 0.05$). **(C)** sodium nitroprusside produces similar vasorelaxation at pH_o 7.4 and 6.8. (D) NO release is increased under acidic pH_o (6.8) vs. pH_o (7.4)**.**

Fig. 2. Percent maximal inhibition by both L-NAME and indomethacin against AIR in NA-pre-contracted SMA is increased under acidosis. (A-B) At pH_o 7.4, both indomethacin and combination of L-NAME and indomethacin inhibit the AIR (**P* < 0.05), but not L-NAME alone. Conversely, during acidosis, all these maneuvers further significantly inhibit the AIR with a shift of the CRC to right (**P* < 0.05, n = 5-9) (C-D).

Fig. 3. Percent maximal inhibition of both L-NAME and indomethacin against AIR in KCl-pre-contracted SMA is increased under acidosis. (A-D) These data demonstrate that the effects of different inhibitors examined are similar to those described above in Fig. 2, except that the % maximal relaxation with AIR was higher in NA-pre-contracted preparations. For that reason, the remaining studies were done in NA-pre-contracted vessels.

Fig. 4. The blocking effect of ODQ and 18β-glycyrrhetinic acid (18β GA) is significantly (*P < 0.05) increased and cGMP pathway is activated under acidosis. Both ODQ (A) and 18β GA (B) significantly attenuate AIR with a rightward shift of CRC at pH_o 7.4 and pH_o 6.8. (**P* < 0.05, n = 6-12.). Maximal percent inhibition of ODQ (C) and 18β GA (D) is significantly

increased under acidosis (*$P < 0.05$, n = 6-12). (E) The cGMP level is increased under acidic pH_o (6.8) vs. pH_o (7.4), which was blocked by BAPTA, AM (1 μM, 10 μM)**.**

Fig. 5. Percent maximal inhibition of both ODQ and 18β GA is increased under acidosis. ODQ (A) and 18β GA (B) significantly inhibit SIR at pH_o 7.4 and pH_o 6.8 (*$P < 0.05$, n = 6-12). The inhibitory effect of ODQ (C) and 18β GA (D) is significantly increased under acidosis (*$P < 0.05$, n = 6-12).

Fig. 6. qPCR and WB data show an increase in connexin expression following acidosis. (A) qPCR analysis for *Cx37, Cx40* and *Cx43* in goat SMA (A), and WB analysis (B-C) in goat SMA showing significant increase in Cx37, Cx43 and iNOS following acidosis (*$P < 0.05$, n = 4).

Fig. 7. Schematic representation of the effect of acidosis on mediators of relaxation in SMA. Acetyl choline binds to muscarinic type 3 receptor (M_3R) in the vascular endothelial cell to activate PLC-IP_3-DAG pathway increasing $[Ca^{2+}]_i$ which then activates eNOS and COX to release NO and PGI_2, respectively. Subsequently, NO and PGI_2 diffuse to the adjacent SMC where they interact with sGC and IP, thus increasing cytosolic cGMP and cAMP, the mediators of vasorelaxation. MEGJ, the channels allowing for the electrical and metabolic coupling between EC and SMC are formed by oligomerization of hexameric connexin to form connexon or hemichannel (HC). Acidosis augments the vasorelaxation by (i) activating eNOS-cGMP, (ii) stimulating COX-2-PGI_2, (iii) opening up the connexon and hemichannels, and (iv) increasing the expression of connexins.

Abbreviations used in figure 7: $[Ca^{2+}]_i$ intracellular Ca^{2+}; 18β-*GA*, 18β-glycyrrhetinic; AA, arachidonic acid; AC, adenylyl cyclase; cAMP, cyclic adenosine monophosphate; cGMP, cyclic guanosine monophosphate; COX, cyclooxygenase; *Cx*, connexin; DAG, diacylglycerol; eNOS,

endothelial nitric oxide synthetase; GJ, gap junction; HC, hemichannels; IP, PGI_2 receptor; IP_3, inositol triphosphate; PGI_2, prostacyclin; MEGJ, myoendothelial gap junctions; M_3R, muscarinic receptor; PGIS, prostacyclin synthetase; sGC, soluble guanylyl cyclase; SER, sarcoplasmic reticulum; PLC, phospholipase C; NO, nitric oxide; L-NAME, L-N^G-nitroarginine methyl ester; ODQ, 1H-[1,2,4]oxadiazolo[4,3-a]quinoxalin-1-one; SMC, smooth muscle cell. Arrows indicate stimulation, and red bars indicate inhibition.

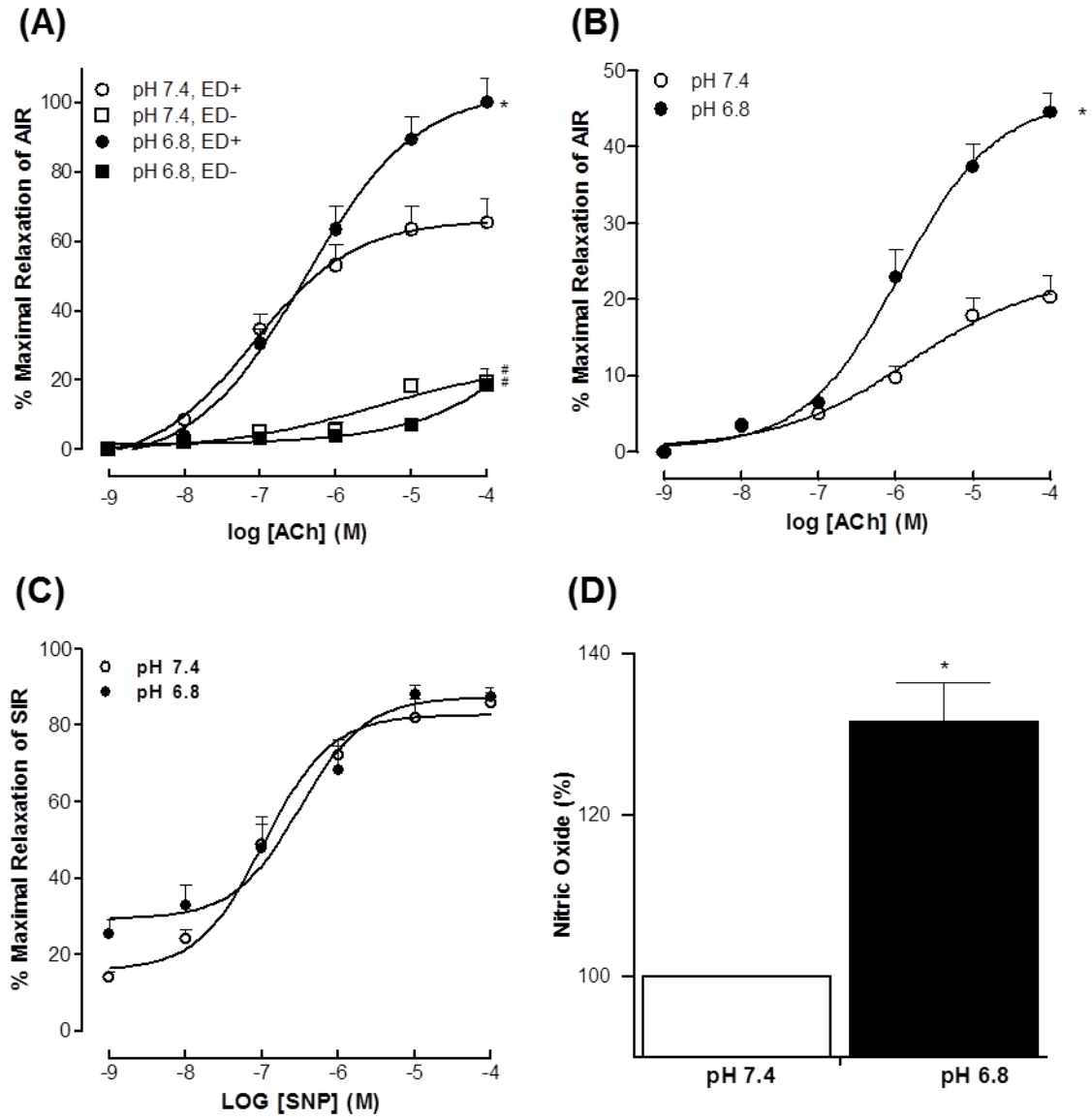
(A)
pH 7.4, ED+
pH 7.4, ED-
pH 6.8, ED+
pH 6.8, ED-
% Maximal Relaxation of AIR
log [ACh] (M)
(B)
pH 7.4
pH 6.8
% Maximal Relaxation of AIR
log [ACh] (M)
(C)
pH 7.4
pH 6.8
% Maximal Relaxation of SIR
LOG [SNP] (M)
(D)
Nitric Oxide (%)
pH 7.4
pH 6.8

Figure 1

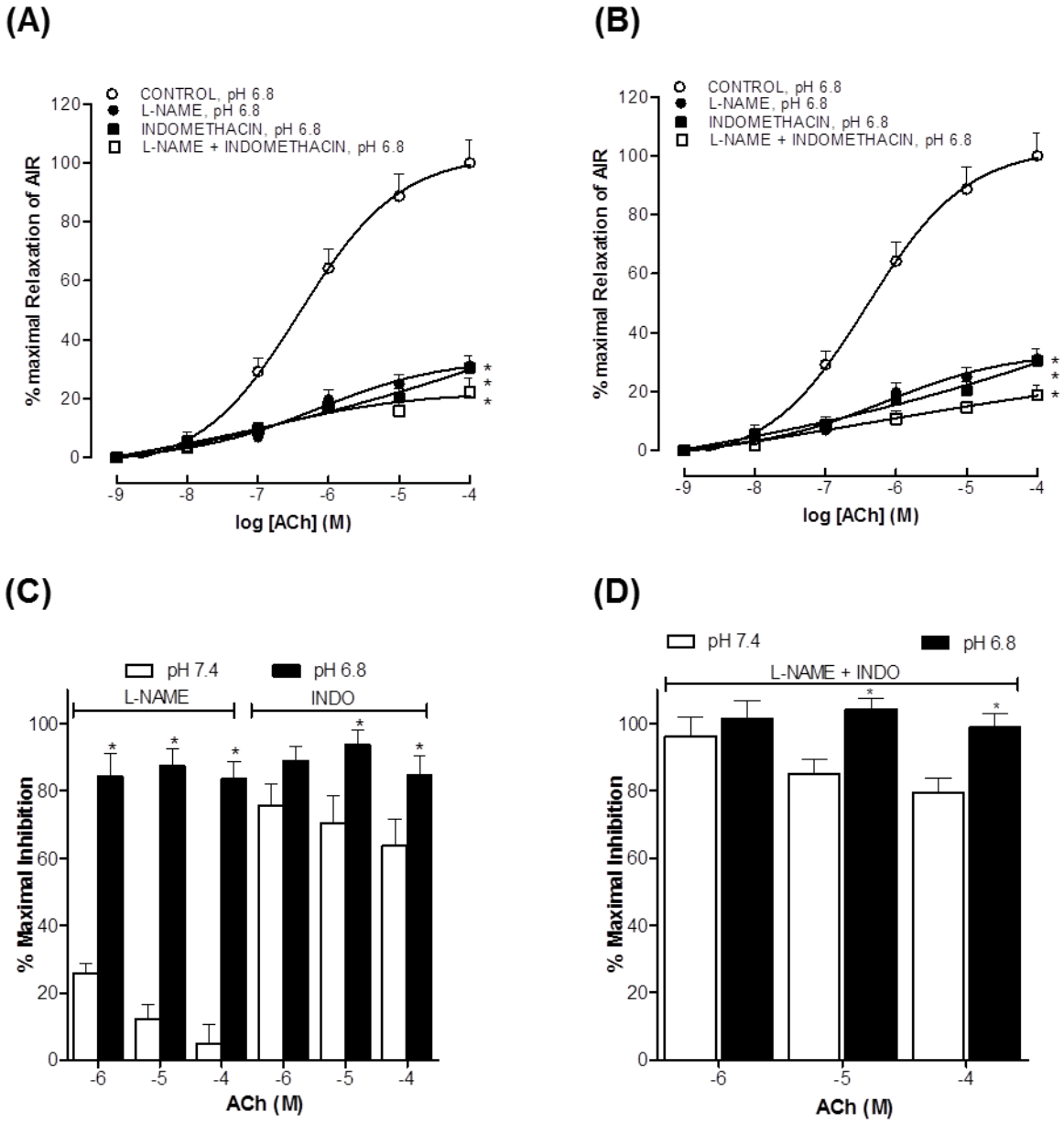
(A)
CONTROL, pH 6.8
L-NAME, pH 6.8
INDOMETHACIN, pH 6.8
L-NAME + INDOMETHACIN, pH 6.8
% maximal Relaxation of AIR
log [ACh] (M)
(B)
CONTROL, pH 6.8
L-NAME, pH 6.8
INDOMETHACIN, pH 6.8
L-NAME + INDOMETHACIN, pH 6.8
% maximal Relaxation of AIR
log [ACh] (M)
(C)
pH 7.4
pH 6.8
L-NAME
INDO
% Maximal Inhibition
ACh (M)
(D)
pH 7.4
pH 6.8
L-NAME + INDO
% Maximal Inhibition
ACh (M)

Figure 2

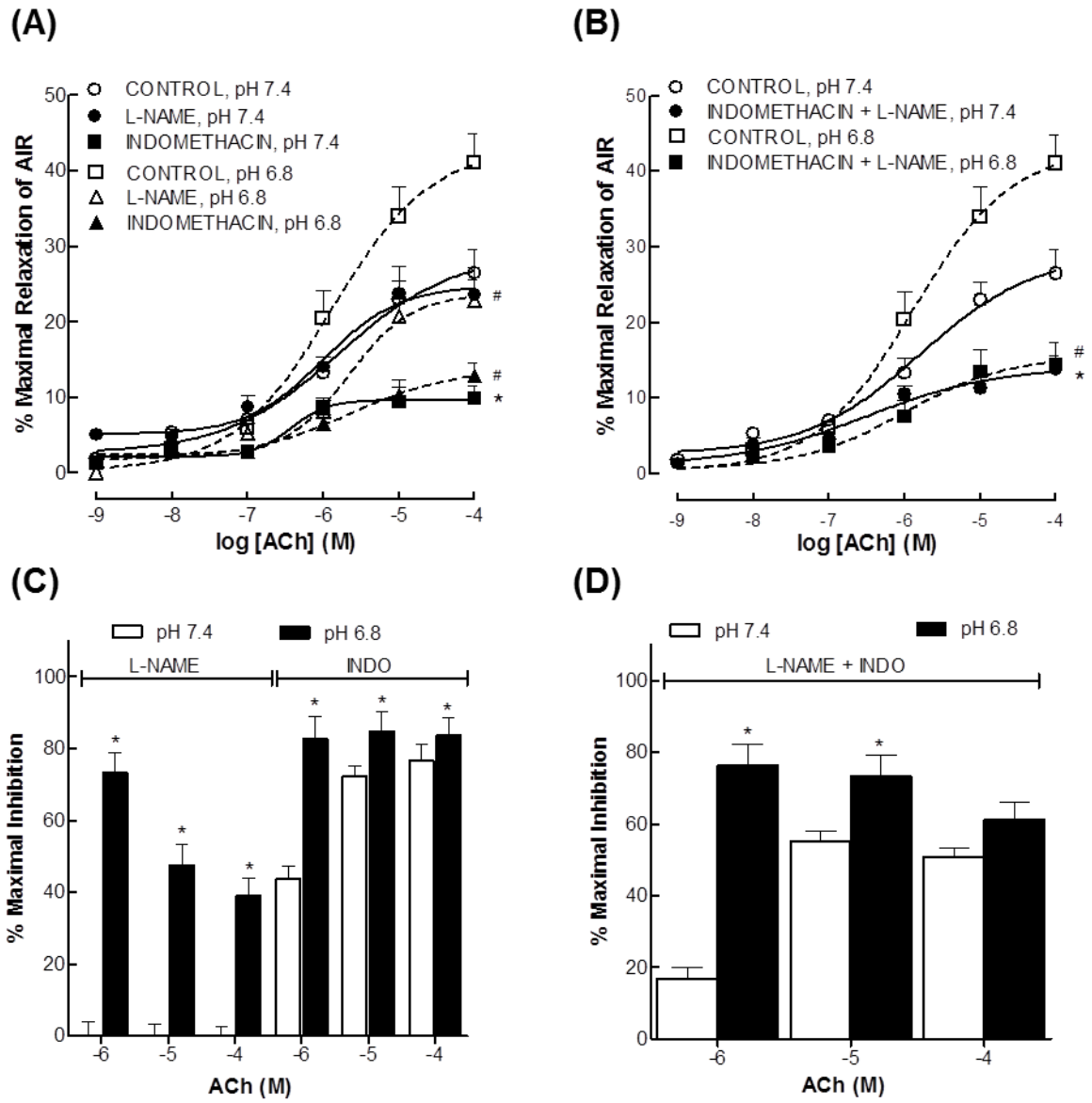
(A)
CONTROL, pH 7.4
L-NAME, pH 7.4
INDOMETHACIN, pH 7.4
CONTROL, pH 6.8
L-NAME, pH 6.8
INDOMETHACIN, pH 6.8
% Maximal Relaxation of AIR
log [ACh] (M)
(B)
CONTROL, pH 7.4
INDOMETHACIN + L-NAME, pH 7.4
CONTROL, pH 6.8
INDOMETHACIN + L-NAME, pH 6.8
% Maximal Relaxation of AIR
log [ACh] (M)
(C)
pH 7.4
pH 6.8
L-NAME
INDO
% Maximal Inhibition
ACh (M)
(D)
pH 7.4
pH 6.8
L-NAME + INDO
% Maximal Inhibition
ACh (M)

Figure 3

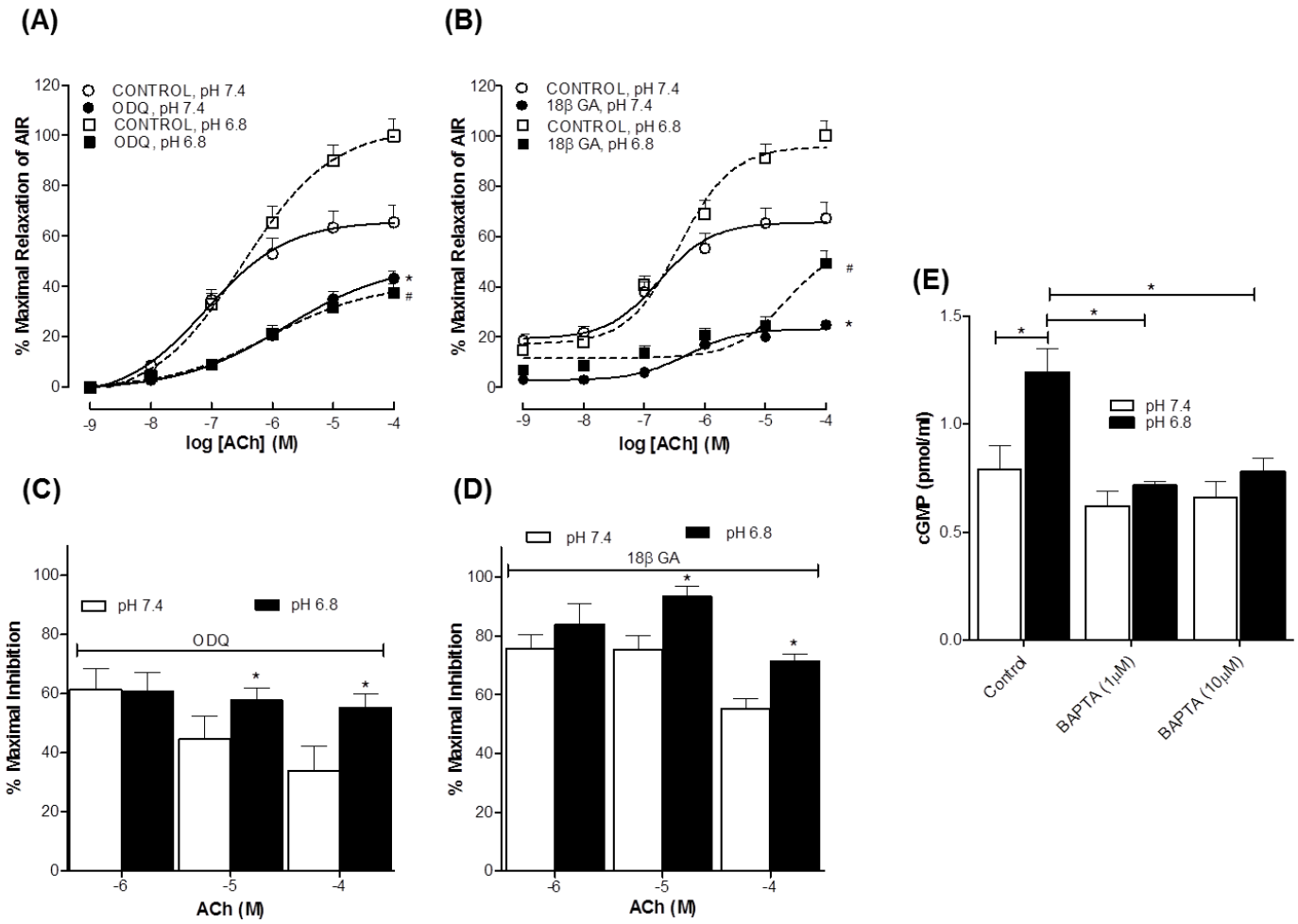
(A)
CONTROL, pH 7.4
ODQ, pH 7.4
CONTROL, pH 6.8
ODQ, pH 6.8
% Maximal Relaxation of AIR
log [ACh] (M)
(B)
CONTROL, pH 7.4
18β GA, pH 7.4
CONTROL, pH 6.8
18β GA, pH 6.8
% Maximal Relaxation of AIR
log [ACh] (M)
(C)
pH 7.4
pH 6.8
ODQ
% Maximal Inhibition
ACh (M)
(D)
pH 7.4
pH 6.8
18β GA
% Maximal Inhibition
ACh (M)
(E)
pH 7.4
pH 6.8
cGMP (pmol/ml)
Control
BAPTA (1μM)
BAPTA (10μM)

Figure 4

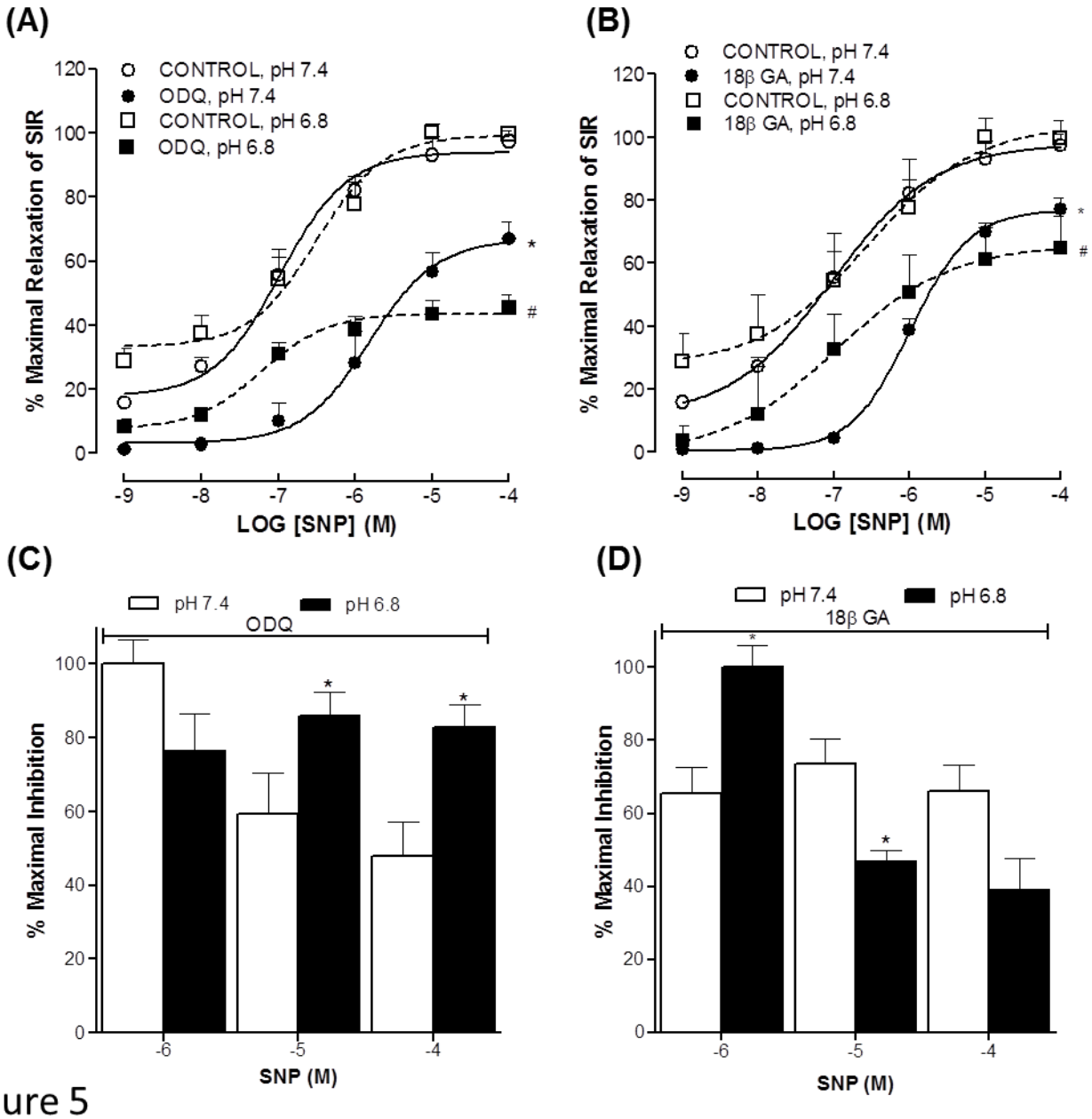
(A)
CONTROL, pH 7.4
ODQ, pH 7.4
CONTROL, pH 6.8
ODQ, pH 6.8
% Maximal Relaxation of SIR
LOG [SNP] (M)
(B)
CONTROL, pH 7.4
18β GA, pH 7.4
CONTROL, pH 6.8
18β GA, pH 6.8
% Maximal Relaxation of SIR
LOG [SNP] (M)
(C)
pH 7.4
pH 6.8
ODQ
% Maximal Inhibition
SNP (M)
(D)
pH 7.4
pH 6.8
18β GA
% Maximal Inhibition
SNP (M)

Figure 5

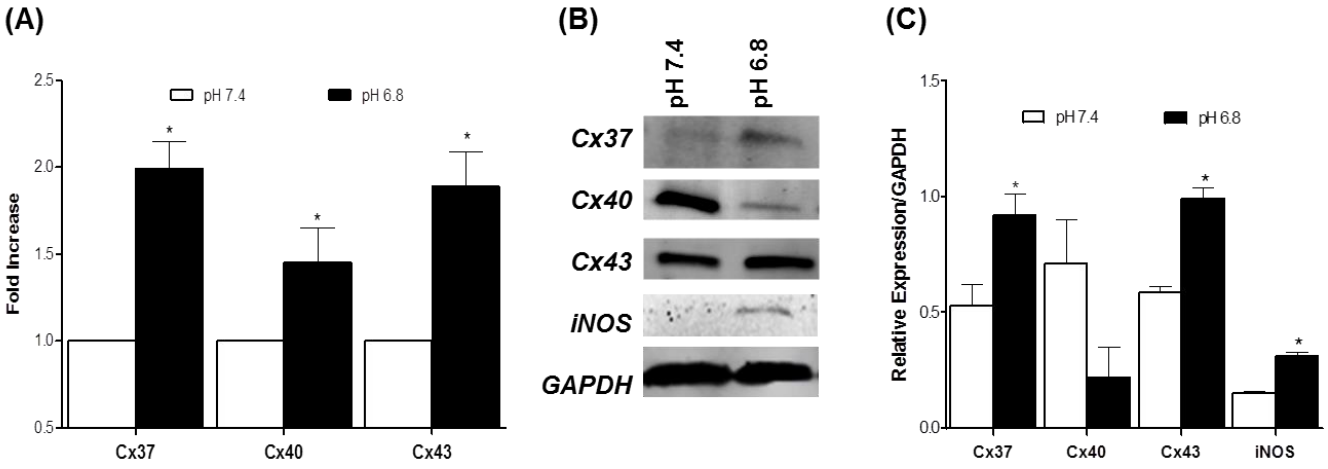
(A)
pH 7.4
pH 6.8
Fold Increase
2.5
2.0
1.5
1.0
0.5
Cx37
Cx40
Cx43
(B)
pH 7.4
pH 6.8
Cx37
Cx40
Cx43
iNOS
GAPDH
(C)
pH 7.4
pH 6.8
Relative Expression/GAPDH
1.5
1.0
0.5
0.0
Cx37
Cx40
Cx43
iNOS

Figure 6

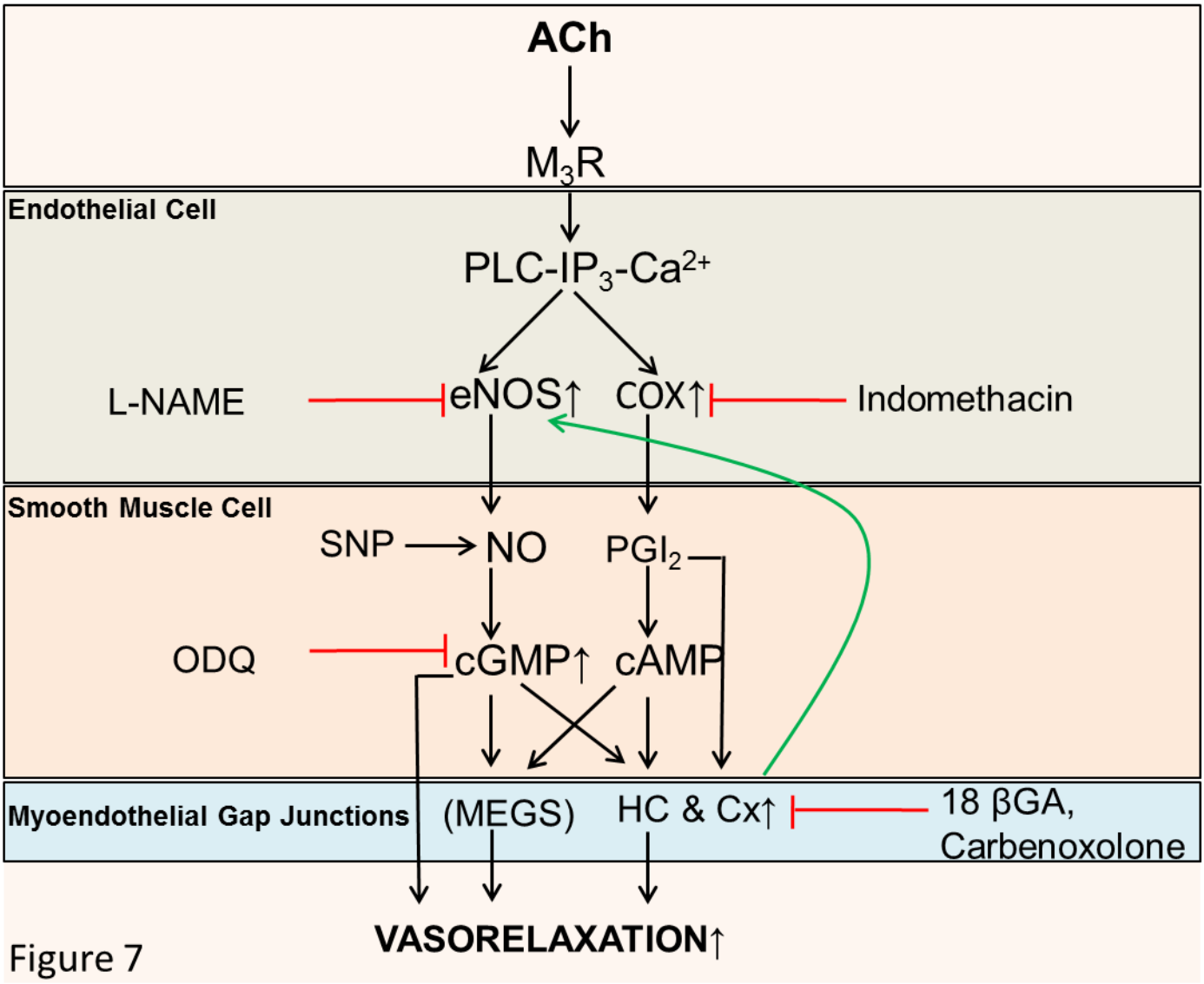
ACh
M3R
Endothelial Cell
PLC-IP3-Ca2+
L-NAME
eNOS↑
COX↑
Indomethacin
Smooth Muscle Cell
SNP
NO
PGI2
ODQ
cGMP↑
cAMP
Myoendothelial Gap Junctions
(MEGS)
HC & Cx↑
18 βGA,
Carbenoxolone
VASORELAXATION↑

Figure 7